

Transition-metal Complexes of Pyrrole Pigments. XIV.¹⁾ An Electron Spin Resonance Study of Bis(3,3',5,5'-tetramethyldipyrromethenato)manganese(II)[†]

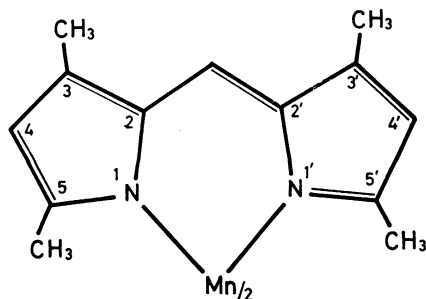
Yoshihisa MATSUDA and Yukito MURAKAMI*

Department of Organic Synthesis, Faculty of Engineering, Kyushu University, Hakozaki, Higashi-ku, Fukuoka 812

(Received April 13, 1977)

Bis(3,3',5,5'-tetramethyldipyrromethenato)manganese(II) in single crystalline and powdered sample states was investigated by means of K-band ESR spectroscopy. The spectral shape for the single crystal depends highly on the angle between the external magnetic field and the crystal axes. Anisotropic parameters D and E evaluated by the simulation method are 0.12 ± 0.01 and 0.032 ± 0.004 cm⁻¹, respectively. These values are considerably larger than those expected for the distorted tetrahedral manganese(II) complexes formed with four equivalent donor atoms. An origin of these large anisotropic parameters has been discussed.

Some bivalent and trivalent manganese complexes of dipyrromethenes were observed previously to show d→d transition bands of unusual high intensity.²⁾ The high transition probabilities can be attributed to mixing of the excited states of different spin-multiplicity into the ground electronic state through the simple spin-orbit coupling interaction, or else to the strong covalent interaction between manganese and aromatic nitrogen atoms. The ground state of high spin manganese(II) complexes should have d-electrons distributed in a manner of spherical symmetry, i.e., it is in the sextet S-like state. Bis(3,3',5,5'-tetramethyldipyrromethenato)-manganese(II) (**1**), referred to TMD-Mn(II) hereafter,



1

shows d→d bands of unusual high intensity ($\epsilon \approx 160$) with some broadening.²⁾ This spectral feature indicates that the above mentioned effects are significant for the complex. The purpose of this paper is to discuss the electronic structure of TMD-Mn(II) and to characterize the anisotropic nature of the ground state by means of ESR spectroscopy applied to both single crystalline and powdered samples.

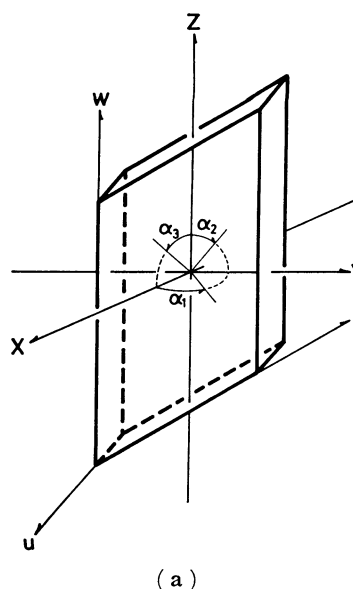
Experimental

The preparative procedure for TMD-Mn(II) has been reported previously.²⁾ Single crystals were grown by cooling down the saturated hexane solution from refluxing to room temperature.

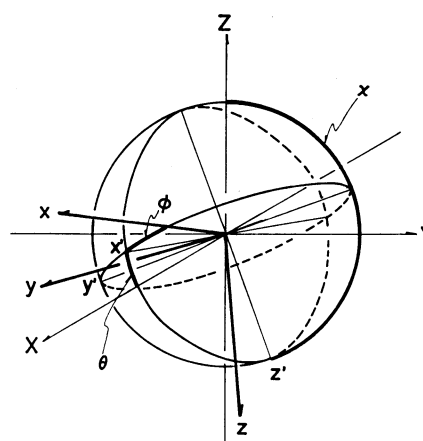
ESR spectra were recorded on a JEOL JES-3K K-band spectrometer, equipped with a 100-kHz field modulation unit and with a modulation amplitude of 20 G, for both single

[†] Contribution No. 400 from this Department.

* To whom correspondence should be addressed.



(a)



(b)

Fig. 1. (a) Correlation between crystal axes (u , v , and w) and experimental axes (X , Y , and Z) about which magnetic field is rotated: $Z \parallel w$, $X \perp vw$ -plane; α_1 , α_2 , and α_3 represent rotation angles about Z , X , and Y , respectively. (b) Correlation between molecular axes (x , y , and z) and conventional axes (X , Y , and Z) defined in Fig. 1a: rotations about X -, y' -, and z -axes by χ , θ , and ϕ (Eulerian angles), respectively, in this sequence convert X , Y , and Z coordinates to x , y , and z .

crystalline and powdered samples. The manganese(II) ion diffused thermally into magnesium oxide was used to provide the reference signals for measurements. The lack of crystallographic data for the single crystal made it difficult to establish *a priori* the relevant axes for ESR measurements in connection with the molecular coordinates. The Cartesian coordinates X , Y , and Z were set up for convenience with respect to the rhombohedral single crystal as shown in Fig. 1a. The crystal axes u , v , and w , defined as shown in Fig. 1a, have no ordinary crystallographic meaning. The Z -axis is parallel to the w -axis, and the X -axis is perpendicular to the vw -plane, while the Y -axis is perpendicular to both X and Z . The single crystal was mounted on a sample holder in a manner that the magnetic field can be applied effectively in a direction perpendicular to one of X , Y , and Z axes, and rotations were performed about these axes for ESR measurements. The rotation angles about these axes (α_1 , α_2 , and α_3) are defined as shown in Fig. 1a.

Computational Procedures

The ordinary ESR signals for the d^5 system are interpreted by the spin Hamiltonian

$$\mathcal{H} = g\beta H \cdot S + D[S_z^2 - S(S+1)/3] + E[S_x^2 - S_y^2] + AS \cdot I + \text{higher order terms} \quad (1)$$

The contribution of higher order terms is usually very small, in fact confirmed to be so in this work, and can be neglected. In addition, the hyperfine term was neglected due to the absence of such hyperfine ESR structures for the present undiluted chelate system. Then, Eq. 1 is simplified as follows for the six spin states ($m_s = 5/2, -5/2$)

$$\mathcal{H} = g\beta H \cdot S + D[S_z^2 - S(S+1)/3] + E[S_x^2 - S_y^2] \quad (2)$$

Computations were performed by substituting sets of D and E values of reasonable magnitude. The level splittings were evaluated by solving the Hamiltonian for every 10° of both θ and ϕ , where θ and ϕ are the polar angles for the direction of magnetic field in the molecular coordinate system (x , y , and z), and the magnetic field intensities at resonance were consequently obtained. The numerical calculations were carried out on a Facom 230-60 computer of the Computer Center of Kyushu University. The anisotropic parameters D and E were obtained roughly from comparison of the ESR spectrum for powdered sample and the calculated resonance positions for the applied magnetic field parallel to the anisotropic axes (molecular axes) as shown in Figs. 3 and 4. The D and E parameters were then reexamined whether or not one set of parameters allows the existence of the corresponding set of reasonable θ , ϕ , and χ values (Fig. 1b), which provide satisfactory elucidation of the ESR spectra for the single crystal.

Results

ESR spectra observed for the single crystal are shown in Fig. 2 for rotation about the Z -axis as an example. The spectra consist of a set of five strong peaks and some weaker ones. Consequently, it is obvious that manganese occupies only a single kind of coordination sites in the unit cell. The spectra depend highly on the rotation angles α_1 , α_2 , and α_3 .

A spectrum for the powdered sample is given in

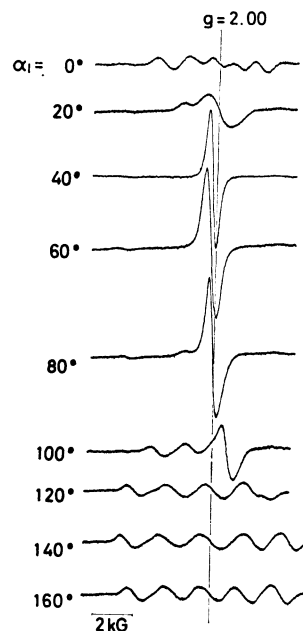


Fig. 2. Single crystal ESR spectra at room temperature (K-band): the magnetic field is rotated about the Z -axis (Fig. 1a) by α_1 .

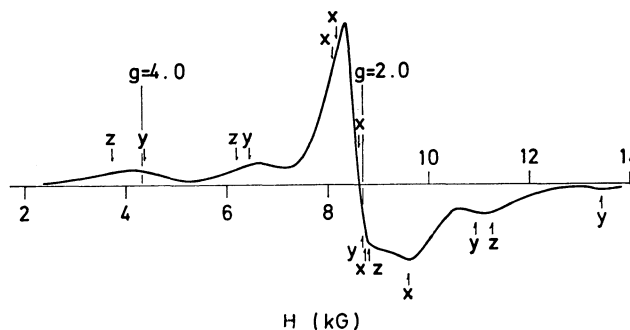


Fig. 3. K-band ESR spectrum of the powdered sample at room temperature. Arrows indicate the predicted resonance positions under the magnetic fields directed along the molecular axes (x , y , and z).

Fig. 3. The spectrum showing a strong peak at $g_{\text{eff}} \approx 2.0$ and weaker one at $g_{\text{eff}} \approx 4.0$ is characteristic of those having anisotropic parameters $D \leq h\nu$ and $E \approx 0.3D$, as clarified by Dowsing and Gibson.³⁾ The correlation between resonance position and E/D is illustrated in Fig. 4 for the cases that the magnetic field is applied parallel to the x , y , and z axes. Upon comparison of this with Fig. 3, the D and E/D values are estimated as 0.12 cm^{-1} and 0.25 , respectively. Resonance positions for magnetic field parallel to the x , y , and z axes are given in Fig. 3 by arrows. The final D and E values evaluated by the computational procedure mentioned in the preceding section are 0.12 ± 0.01 and $0.032 \pm 0.004 \text{ cm}^{-1}$, respectively (refer to Figs. 5 and 6).

The computational results due to the manipulation of Eq. 2 are given in Fig. 5 as the correlation between resonance magnetic field and polar coordinates θ and ϕ . The allowed transitions ($\Delta m_s = 1$) are denoted by solid lines, and the forbidden transitions with $\Delta m_s = 2$ and $\Delta m_s > 2$ are represented by broken lines, respectively.

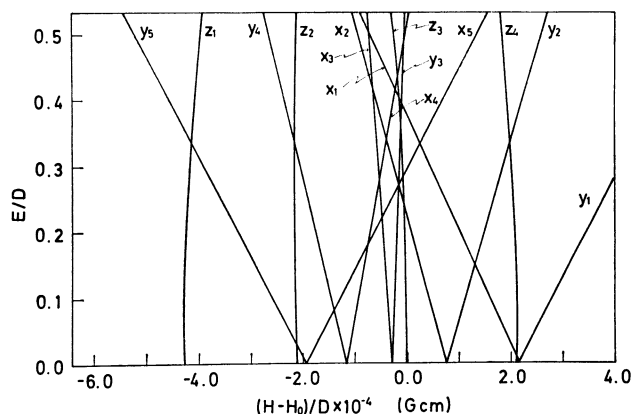


Fig. 4. Correlation between zero-field splitting parameters and resonance positions: $H_0 = h\nu/g_0\beta$. Suffix numbers refer to the transitions: 1, $-5/2 \leftrightarrow -3/2$; 2, $-3/2 \leftrightarrow -2/2$; 3, $-1/2 \leftrightarrow 1/2$; 4, $1/2 \leftrightarrow 3/2$; 5, $3/2 \leftrightarrow 5/2$.

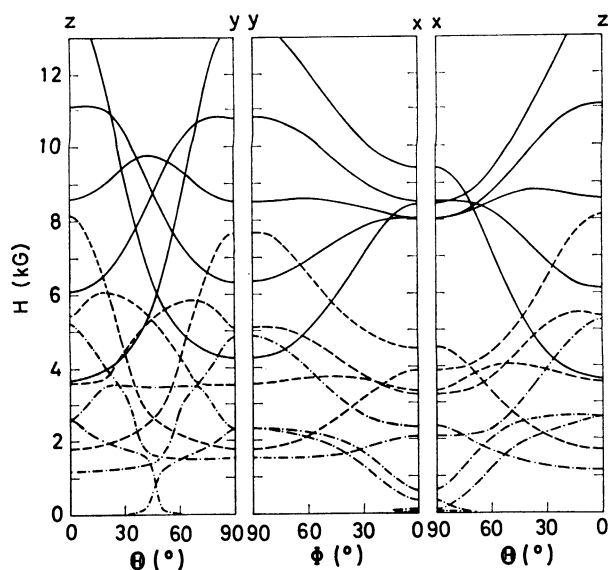


Fig. 5. Predicted ESR transitions for $S=5/2$ with $D=0.12 \text{ cm}^{-1}$, $E=0.032 \text{ cm}^{-1}$, and $h\nu=0.81 \text{ cm}^{-1}$: —, transitions for $\Delta m_s=1$; ----, transitions for $\Delta m_s=2$; - · - · -, transitions for $\Delta m_s > 2$. θ , polar angle between z-axis and magnetic field; ϕ , polar angle between x-axis and magnetic field projected on xy-plane.

Subsequently, the Eulerian angles θ , ϕ , and χ were evaluated as 7.7° , 43.3° , and 153.0° , respectively. The calculated correlations between resonance positions and rotation angles (α_1 , α_2 , and α_3) are illustrated in Fig. 6 along with the experimental results. The agreements between calculated and experimental data are quite satisfactory.

Discussion

Several investigators have reported on the coordination structures of manganese(II) complexes in which the central metal is subject to either regular or distorted tetrahedral ligand field. Since the bivalent manganese is in general favorably placed in the octahedral ligand

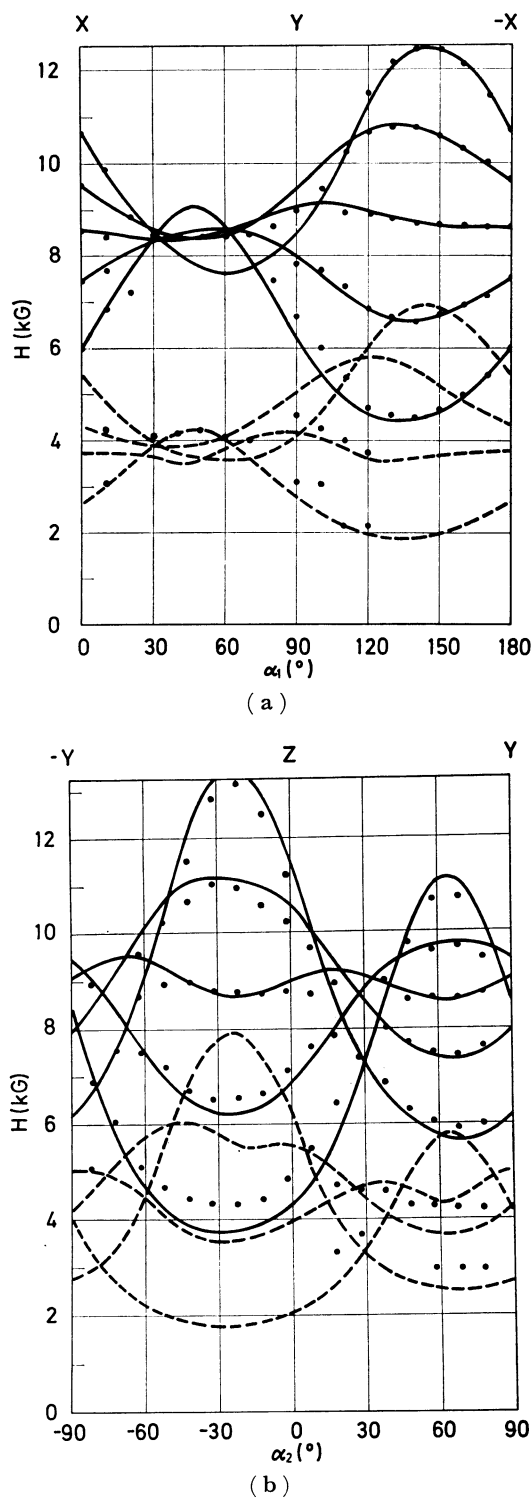
field, the steric effect may provide primarily a cause for the tetrahedral coordination. Moreover, the distorted tetrahedral coordination is less common for this metal ion. Most of these distortions have been caused by the structural nature of host lattice, which gives a geometrically distorted configuration of four equivalent donor atoms.⁴ The rest has been due to the intramolecular repulsive interaction among ligands, where the coordination of electronically different donor atoms takes place. In those cases, the configuration of donor atoms is close to the regular tetrahedron. The anisotropic parameters D and E for manganese(II) placed in those geometrically distorted ligand fields are very close to zero and the corresponding g -value is nearly the free electron value.⁴

On the other hand, the tetrahedral manganese(II) complexes are reported to be subject to the profoundly large anisotropy in a few cases.⁵ In those cases, two kinds of electronically different donor atoms are involved for the formation of a complex. Nevertheless, the mechanism responsible for the occurrence of this large anisotropy has not been clearly elucidated. Some iron(III) complexes show anisotropy larger than manganese(II) complexes. Cole and Garrett studied the large anisotropy of the aquapentachloroiron(III) anion, and attributed the origin of the large D value to the tetragonal distortion of coordination geometry.⁶

Judging from the existence of nonzero D and E values, TMD-Mn(II) is obviously in a distorted tetrahedral coordination structure. The electronic property is, however, identical with each other among all the four nitrogen donor atoms due to the resonance interaction within each dipyrromethene molecule. In any case, the bulky methyl groups placed at the 5- and 5'-positions in the present ligand hinder the planar alignment of four nitrogen atoms. Since there is no significant steric reason against attaining the regular tetrahedral geometry, manganese(II) must assume this coordination geometry unless other factors come into play. When the coordinate bonds between manganese(II) and nitrogen atoms attain highly covalent character, the configuration of nitrogen donor atoms can be expected to deviate from the regular tetrahedron toward the planar structure. These effects have been observed for dipyrromethene complexes of transition metals having a partially filled d-shell.⁷

The small D and E values for the geometric distortion can be explained in terms of the splitting of the sextet ground state caused by higher order perturbation due to spin-orbit coupling. On the other hand, TMD-Mn(II) gained the uniquely large D and E values for the complex having four equivalent donor atoms. These large D and E values may be attributed to the strong σ -bonding interaction. The existence of profound σ -bonding between manganese and nitrogen atoms tends to distort the coordination geometry from tetrahedral toward tetragonal, causing the mixing of the excited quartet into the sextet ground state. The π -bonding interaction between the central metal atom and the ligand molecules may be partly responsible for such tetragonal distortion.

In conclusion, the eminent covalent interaction between manganese(II) and donor atoms caused the



distortion of ligand alignment from the regular tetrahedron, and gives out the nonspherical distribution of d-orbitals. The latter effect is accompanied with spin-orbit interaction with the excited configurations. This

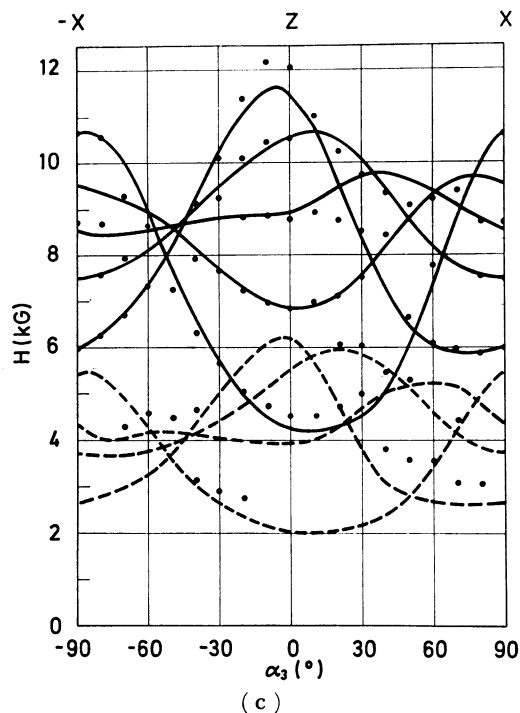


Fig. 6. Resonance positions for single crystal under the magnetic field rotated by α_1 (a), α_2 (b), and α_3 (c) (refer to Fig. 1a). Solid and broken lines denote the calculated resonance positions ($\Delta m_s = \pm 1$ and ± 2 , respectively) for $D=0.12$ cm^{-1} , $E=0.032$ cm^{-1} , and $h\nu=0.81$ cm^{-1} , and solid circles indicate the observed values.

mechanism must be responsible for the profound anisotropy existing in the N_4 -pseudotetrahedral manganese complex, as well as for the exceedingly high intensity of ligand field bands due to spin forbidden transitions.²⁾

References

- 1) Part XIII: Y. Murakami and Y. Aoyama, *Bull. Chem. Soc. Jpn.*, **49**, 683 (1976).
- 2) Y. Murakami, K. Sakata, K. Harada, and Y. Matsuda, *Bull. Chem. Soc. Jpn.*, **47**, 3021 (1974).
- 3) R. D. Dowsing and J. F. Gibson, *J. Chem. Phys.*, **50**, 294 (1969).
- 4) For example: P. B. Dorain, *Phys. Rev.*, **112**, 1058 (1958).
- 5) R. D. Dowsing, J. F. Gibson, D. M. L. Goodgame, M. Goodgame, and P. J. Hayward, *J. Chem. Soc., A*, **1969**, 1242.
- 6) G. M. Cole, Jr. and B. B. Garrett, *Inorg. Chem.*, **13**, 2680 (1974).
- 7) (a) Y. Murakami, Y. Matsuda, and K. Sakata, *Inorg. Chem.*, **10**, 1728 (1971); (b) Y. Murakami, Y. Matsuda, and K. Sakata, *ibid.*, **10**, 1734 (1971).